

Preserving Finite-Volume Schemes for Two-Time Reaction-Diffusion Model

A. El Harrak* and A. Bergam

MAE2D laboratory, Polydisciplinary Faculty of Larache, Abdelmalek Essaadi University, Larache, Morocco

Received: 7 Oct. 2018, Revised: 2 Jul. 2019, Accepted: 6 Jul. 2019

Published online: 1 Jan. 2020

Abstract: In this paper, we propose an auto adaptive time-step finite volume scheme for a class of two-time reaction-diffusion models of spatially structured population dynamics. Under specific assumptions, we prove that the privileged scheme preserves, at the discrete level, the main features of the continuous problem, namely the non-negativity of the solutions, monotonicity and boundedness. Finally, we present some numerical results to illustrate the efficiency of the proposed algorithm and the behaviour of the model and of the scheme.

Keywords: Two time scales, Reaction-diffusion equations, Finite volume method, Adaptive time step

1 Introduction

Recently, there has been a lot of interest in spatial dynamics of ecological systems (see [1–3], among others). Ecological modellers, supported by the fast development of computers, produce a new generation of ecological models with more complexity and details, leading to large dynamical systems involving lots of variables, and thus hard to handle analytically. In population dynamics, as a branch of ecology, we often examine the asymptotic behavior of the dynamics of those models to describe population distribution in the long term (extinction, coexistence, or extinction of species and coexistence of others). Thus, there is a need to present a practical algorithm in terms of computational cost for the numerical resolution of such model to extract mainly information about its dynamics without losing the accuracy of simulations. Indeed, if we use a fixed-time algorithm, we will either do a lot of useless calculations or lose the main features of the numerical solution. Therefore, the use of an adaptive algorithm is inevitably required in order to reduce the computational cost without losing the accuracy of solutions.

Adaptive strategy is becoming an important issue in many areas of engineering. In other words, a large number of theoretical results and numerical experiments provided in many studies suggesting its viability and efficiency for practical calculations. In the literature, we

find different types of adaptive algorithms; in space, time, and both in space and time. Adaptive algorithms in space, that are often based on a posteriori error estimation techniques, have become an indispensable tool in large scale scientific computation and a lot of studies have been done for different discretization techniques of many problems (see for instance [4–7]). Also, adaptive time stepping is an important tool to find an approximate solution in terms of computational cost. It helps to control the error and the accuracy of simulations and allows preserving the main features of the continuous solution as well, more particularly existence, uniqueness, stability, non-negativity and boundedness.

Many formulas have been presented to introduce a time-step size control for error in a lot of work in adaptive algorithm framework. An adaptive time step control could be used either for controlling error or for preserving main features [8, 9]. As far as controlling error is concerned it needs some error indicator which the next time step length is based on. This error indicator proposes a new time step size to achieve a given accuracy. However, the adaptive time-step for controlling main features is based on the auto determination of a time-step that ensures the preservation of the main features of continuous solution.

In this paper, we are interested in properties of the approximate solution to a two-time reaction-diffusion equation of spatially structured population dynamics, and

* Corresponding author e-mail: anouarelharrak1@gmail.com

we aim at proposing an auto adaptive time-step algorithm for preserving main features of finite volume scheme.

Finite volume method is a discretization method in space, which is appropriate for the numerical simulation of various types of conservation laws e.g elliptic, parabolic or hyperbolic, [10–13]. It may be used on arbitrary geometries; structured or unstructured meshes, and it accordingly leads to robust schemes. The choice of this method for our problem is due to the conservative aspect of the method that is suitable for the conservation law of our problem (3) (see [14–16]).

The rest of the paper is organized as follows; the problem is introduced in Section 2. In Section 3, we define some notations for the finite volume discretization, and we present our proposed scheme. In section 4, we introduce the existence, uniqueness and main features of solutions to the discrete problem. Finally, we implement an auto adaptive time step algorithm that ensures L^∞ -stability of the mentioned scheme and preserves the main features of the approximate solution, and then numerical results are provided to illustrate the behavior of the scheme and the efficiency of the implemented algorithm, in Section 5.

2 Statement of the problem

An accurate description of systems in population dynamics requires a combination of different processes that are often linked to multiple time scales (see [17, 18]). In this work, we consider a two-time reaction-diffusion model of spatially structured population dynamics which governs the evolution of a population n . Population density $n(x, t)$ at position x and at time t is subjected to diffusion and local demography (growth, mortality, etc.). The diffusion takes place at a faster time scale than local growth, whose dynamics at a fast time scale is

$$\frac{\partial n}{\partial s}(x, s) = \operatorname{div}(D(x)\nabla n(x, s)) + \varepsilon f(x, n(x, s)). \quad (1)$$

The first and the second terms of the second member describe, respectively, the fast and slow processes. The parameter ε is a small positive constant representing the ratio between time scales.

We note s and $t = \varepsilon s$, respectively, the time variable in the fast and the slow time units. Then, a change of time scales is performed in order to use them explicitly in the model. Re-scaling the time as $t = \varepsilon s$ in Eq. (1), we obtain the dynamics at a slow time scale:

$$\frac{\partial n_\varepsilon}{\partial t}(x, t) = \frac{1}{\varepsilon} \operatorname{div}(D(x)\nabla n_\varepsilon(x, t)) + f(x, n_\varepsilon(x, t)). \quad (2)$$

We consider a population living in a spatial region $\Omega \subset \mathbb{R}^p$ ($p \geq 1$) where Ω is a non-empty bounded, open and connected set with smooth boundary $\partial\Omega \in C^k$, $k \geq 1$.

We assume that the demography is given by a nonlinear reaction term $f(x, n)$ that satisfies the following regularity conditions:

Hypothesis 1. *The function $f : \overline{\Omega} \times \mathbb{R} \rightarrow \mathbb{R}$ is continuous, and there exists a real-valued continuous positive function h defined on $\overline{\Omega} \times \mathbb{R} \times \mathbb{R}$ such that:*

$$|f(x, u) - f(x, v)| \leq h(x, u, v) |u - v|, \quad \forall x \in \overline{\Omega}, \quad \forall (u, v) \in \mathbb{R}^2$$

We also assume a linear diffusion process in Ω for the population, with coefficient $D \in C^2(\overline{\Omega})$, $D(x) \geq d^* > 0$, that occurs at a fast time scale. We consider the following two-time reaction-diffusion equation for the population density:

$$\begin{cases} \frac{\partial n_\varepsilon}{\partial t}(x, t) = \frac{1}{\varepsilon} \operatorname{div}(D(x)\nabla n_\varepsilon) + f(x, n_\varepsilon), & x \in \Omega, t > 0 \\ \frac{\partial n_\varepsilon}{\partial \nu}(x, t) = 0, & x \in \partial\Omega, t > 0 \\ n_\varepsilon(x, 0) = n_0(x), & x \in \Omega \end{cases} \quad (3)$$

where Neumann boundary condition indicates that the spatial domain is isolated from the external environment.

In addition, we suppose the following condition that is sufficient to eliminate blow-up of non-negative solutions:

Hypothesis 2. *The function $f : \overline{\Omega} \times \mathbb{R} \rightarrow \mathbb{R}$ satisfies the following:*

$$i) f(x, 0) = 0, \quad \forall x \in \overline{\Omega}$$

ii) *There exists a constant $C_f > 0$ such that $\forall x \in \overline{\Omega}$ and $\forall u \in \mathbb{R}$ with $|u| \geq C_f$, we have $f(x, u) \leq 0$.*

The previous hypotheses are ecologically feasible. Indeed, the population grows nowhere indefinitely; its growth is limited by the finite amount of food available for example. Also, there is no spontaneous generation of individuals.

The existence and boundedness of global non-negative solutions to the problem (3) are proved in [19]. Assuming the previous hypotheses and the additional ones, we will prove that numerical solution to (3), obtained by using a finite volume method, preserves the non-negativity, monotonicity and boundedness of its exact one.

3 Finite Volume discretization

In this section, we will present a finite volume scheme applied to the problem (3). Since the problem (3) arises from conservation laws we will establish an approximation of equation by using a vertex-centered finite volume method. The finite volume scheme is obtained by integrating the equation of the problem on a given control volume of a mesh discretization, and by the divergence formula we obtain an integral formulation of the flux on the boundary which will be discretized with respect to the discrete unknowns (see [12, 20, 21]).

Let Ω be an open polygonal bounded subset of \mathbb{R}^p , with $p = 2$ or $p = 3$, and $T > 0$ fixed. We denote $\mathcal{T}_h = (K)_{K \in \mathcal{T}_h}$ a regular triangulation of Ω with $h = \max h_K$ and h_K is the diameter of the triangle K of

\mathcal{T}_h . The partition \mathcal{T}_h satisfies that there exists a positive constant $C > 0$ such that

$$C^{-1}h^2 \leq |K| \leq Ch^2, \forall K \in \mathcal{T}_h,$$

$|K|$ is the Lebesgue measure of the triangle K . We denote \mathcal{V}_h the dual partition of Ω , that is based on the triangulation \mathcal{T}_h and formed by control volumes $(V)_{i=1,\dots,M}$, $M = \text{card}(\mathcal{V}_h)$, obtained by connecting the midpoints of the edges of \mathcal{T}_h and circumcenters of each neighbouring triangles having x_V as a vertex (see Fig. 1).

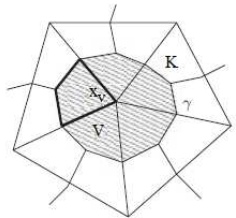


Fig. 1: Vertex centered control volume

We denote by $\mathcal{E}_{\mathcal{T}}$ the set of interior edges γ of \mathcal{T}_h and \mathcal{E}_V the set of interior edges of the dual decomposition \mathcal{V}_h .

To simplify, we set $n_\varepsilon = u$. Integrating (3) over each control volume V of \mathcal{V}_h , we write

$$\int_V \frac{\partial u}{\partial t}(x,t) dx - \frac{1}{\varepsilon} \int_V \text{div}(D(x)\nabla u(x,t)) dx = \int_V f(x,u(x,t)) dx. \quad (4)$$

The time discretization may be performed with a variable time step; we introduce a partition of the interval $[0, T]$ into sub-intervals $[t_n, t_{n+1}]$, $n \in \mathbb{N}^*$ and $0 \leq n \leq N - 1$, such that $0 = t_0 < t_1 < \dots < t_N = T$. We denote by τ_n the length $t_{n+1} - t_n$.

As it is known, the stability condition for an explicit time discretization of a parabolic equation requires the time step to be limited by a power two of the space step, which is generally a too strong condition in terms of computational cost. Therefore, a semi-implicit time discretization is highly required. It is obtained by taking $t = t_{n+1}$ in the left hand side of (4) to rise up the large diffusivity of the problem, and replacing $\partial u / \partial t(x, t)$ by

$$\frac{\partial u}{\partial t}(x,t) \approx \frac{u^{n+1}(x) - u^n(x)}{\tau_n}.$$

For the right hand side of (4) we take $f(x, u^n(x))$. This gives :

$$\int_V \frac{u^{n+1}(x) - u^n(x)}{\tau_n} dx - \frac{1}{\varepsilon} \int_V \text{div}(D(x)\nabla u^{n+1}(x)) dx = \int_V f(x, u^n(x)) dx.$$

Applying Green's formula, we obtain

$$\int_V \frac{u^{n+1}(x) - u^n(x)}{\tau_n} dx - \frac{1}{\varepsilon} \sum_{\gamma \in \partial V \cap \mathcal{E}_V} \int_\gamma D(x)\nabla u^{n+1}(x) \cdot \vec{n}_\gamma ds = \int_V f(x, u^n(x)) dx, \quad (5)$$

where \vec{n}_γ denotes the unit outer-normal vector on the boundary ∂V .

We denote by u_V^{n+1} , $0 \leq n \leq N - 1$ and $V \in \mathcal{V}_h$, an approximation of u in control volume V and at time t_{n+1} , satisfying:

$$\frac{|V|}{\tau_n} (u_V^{n+1} - u_V^n) - \frac{1}{\varepsilon} \sum_{\gamma \in \partial V \cap \mathcal{E}_V} \int_\gamma D(x)\nabla u^{n+1}(x) \cdot \vec{n}_\gamma ds = |V| f_V(u_V^n), \quad (6)$$

with $f_V(u_V^n) = f(x_V, u_V^n)$.

For each control volume $V \in \mathcal{V}_h$, we denote by γ the common edge between the control volume V and its neighboring one W . We use a centered finite difference approximation for the flux $\int_\gamma D(x)\nabla u^{n+1}(x) \cdot \vec{n}_\gamma ds$, we have:

$$\int_\gamma D(x)\nabla u^{n+1}(x) \cdot \vec{n}_\gamma ds \approx \frac{|\gamma|}{d_\gamma} \bar{D}_\gamma (u_W^{n+1} - u_V^{n+1}), \quad (7)$$

where \vec{n}_γ denotes the unit normal vector on the edge γ , $(u_V^{n+1})_{V \in \mathcal{V}_h}$ are the discrete unknowns, d_γ is the distance between x_V and x_W , $|\gamma|$ is the Lebesgue measure of the edge γ and

$$\bar{D}_\gamma = \frac{D(x_V) + D(x_W)}{2}.$$

Using the flux approximation (7) in (6) and taking into account Neumann boundary condition, we obtain

$$\frac{|V|}{\tau_n} (u_V^{n+1} - u_V^n) - \frac{1}{\varepsilon} \sum_{\gamma \in \partial V \cap \mathcal{E}_V} \frac{|\gamma|}{d_\gamma} \bar{D}_\gamma (u_W^{n+1} - u_V^{n+1}) = |V| f_V(u_V^n).$$

Hence, bearing in mind the initial condition yields the following semi-implicit finite volume scheme for the discretization of (3):

$$\frac{|V|}{\tau_n} (u_V^{n+1} - u_V^n) - \frac{1}{\varepsilon} \sum_{\gamma \in \partial V \cap \mathcal{E}_V} \frac{|\gamma|}{d_\gamma} \bar{D}_\gamma (u_W^{n+1} - u_V^{n+1}) = |V| f_V(u_V^n), \quad (8)$$

for all $V \in \mathcal{V}_h$ and $n \in \{0, \dots, N-1\}$.

Initial conditions can be taken into consideration in different ways, depending on the regularity of the data u_0 . It is possible to take

$$u_V^0 = \frac{1}{|V|} \int_V u_0(x) dx, \quad V \in \mathcal{V}_h,$$

or

$$u_V^0 = u_0(x_V), \quad V \in \mathcal{V}_h. \quad (9)$$

The finite volume scheme (8) could be written as a linear system as follows:

$$AU^{n+1} = b^n, \quad n \in \{0, \dots, N-1\},$$

where $b^n = (b_V^n)_{V \in \mathcal{V}_h}$ and $b_V^n := u_V^n + \tau_n f_V(u_V^n)$, A is a square matrix.

Generally, semi-implicit scheme is an appropriate one to find an approximate solution in terms of computational cost, because it leads to a linear system that is very easy to implement, and takes less execution time. However, implicit finite volume scheme leads to a non-linear system that generally requires numerical methods to solve it; those methods are time consuming and their convergence is not ensured, especially for large system.

4 Study of semi-implicit finite volume scheme

We proceed, in this section, to study semi-implicit finite volume scheme (8) by concentrating on non-negative approximate solution. Moreover, we give a monotonicity result, a L^∞ -estimate and global existence of non-negative approximate solution.

4.1 Existence and uniqueness

Lemma 1. *Let Ω be an open polygonal bounded subset of \mathbb{R}^p . Assuming (1) and (2), there exists a unique approximate solution $(u_V^{n+1})_{V \in \mathcal{V}_h}$ satisfying (8) for a given $(u_V^n)_{V \in \mathcal{V}_h}$ with (9).*

Proof. Equations of the semi-implicit scheme (8) for a given $(u_V^n)_{V \in \mathcal{V}_h}$ lead to a linear system of M equations with M unknowns, $(u_V^{n+1})_{V \in \mathcal{V}_h}$. Since $(u_V^{n+1})_{V \in \mathcal{V}_h}$ satisfies this linear system (8) we can write:

$$AU^{n+1} = b^n,$$

where $b^n = (b_V^n)_{V \in \mathcal{V}_h}$ and $b_V^n := u_V^n + \tau_n f_V(u_V^n)$, A is a square matrix $M \times M$.

To ensure the existence and uniqueness of solution $(u_V^{n+1})_{V \in \mathcal{V}_h}$ to (8), we prove that A is positive definite matrix. Multiplying the linear part of each equation with

respect to $(u_V^{n+1})_{V \in \mathcal{V}_h}$ in (8) by u_V^{n+1} , and summing all equations over V , we get

$$L = \sum_{V \in \mathcal{V}_h} |V| (u_V^{n+1})^2 - \frac{\tau_n}{\varepsilon} \sum_{V \in \mathcal{V}_h} \sum_{\gamma \in \partial V \cap \mathcal{E}_\gamma} \frac{|\gamma|}{d_\gamma} \overline{D}_\gamma (u_W^{n+1} - u_V^{n+1}) u_V^{n+1}.$$

Reordering the summation over the set of the interior edges and thanks to the conservation of the flux on each interior edge, we get

$$L = \sum_{V \in \mathcal{V}_h} |V| (u_V^{n+1})^2 + \frac{\tau_n}{\varepsilon} \sum_{\gamma \in \mathcal{E}_\gamma} \frac{|\gamma|}{d_\gamma} \overline{D}_\gamma (u_W^{n+1} - u_V^{n+1})^2.$$

The positivity of the function D completes the proof of the existence and uniqueness of solution to (8).

4.2 Non-negativity, monotonicity and boundedness

The study of some properties of the approximate solution such as non-negativity, monotonicity and boundedness, needs additional hypothesis on the time step length τ_n giving what follows,

Hypothesis 3. *We assume that the time step τ_n in the semi-implicit finite volume scheme (8) should satisfy the following:*

$$\tau_n < \tau_n^{\max}, \quad \forall n \in \{0, \dots, N-1\},$$

where τ_n^{\max} presents a time step size limit at the $(n+1)$ -th iteration.

In our model, the time step influences the features of the approximate solution; if time steps τ_n are chosen less than τ_n^{\max} the approximate solution preserves the non-negativity, monotonicity and boundedness of the continuous one. We notice that the preservation of each property may require a specific assumption on time step length τ_n .

For $(u_V^n)_{V \in \mathcal{V}_h} \in \mathbb{R}^M$ and $(w_V^n)_{V \in \mathcal{V}_h} \in \mathbb{R}^M$, $n \in \{0, \dots, N\}$, we denote by

$$\Theta_{u^n, w^n} = \sup_{V \in \mathcal{V}_h} h(x_V, u_V^n, w_V^n),$$

where h is the function defined in Hypothesis 1.

In the following lemma, we give some results about non-negativity of approximate solution:

Lemma 2. *Let Ω be an open polygonal bounded subset of \mathbb{R}^p . Under the assumptions (1), (2), (3) with $\tau_n^{\max} = \Theta_{u^n, 0}^{-1}$, $\forall n \in \{0, \dots, N-1\}$, and if the vector of the initial data $(u_V^0)_{V \in \mathcal{V}_h}$ satisfies $u_V^0 \geq 0$, $\forall V \in \mathcal{V}_h$. Then the approximate solution $(u_V^{n+1})_{V \in \mathcal{V}_h}$ of (8) verifies*

$$u_V^{n+1} \geq 0, \quad \forall V \in \mathcal{V}_h \text{ and } \forall n \in \{0, \dots, N-1\}.$$

Proof. Let us assume that $u_V^n \geq 0, \forall V \in \mathcal{V}_h$ and prove that

$$u_V := u_V^{n+1} \geq 0, \forall V \in \mathcal{V}_h.$$

For this, we multiply (8) by $(u_V^{n+1})^-$ and sum over V , we get:

$$\begin{aligned} \sum_{V \in \mathcal{V}_h} |V| u_V u_V^- - \frac{\tau_n}{\varepsilon} \sum_{V \in \mathcal{V}_h} \sum_{\gamma \in \partial V \cap \mathcal{E}_\gamma} \frac{|\gamma|}{d_\gamma} \bar{D}_\gamma (u_W - u_V) u_V^- \\ = \sum_{V \in \mathcal{V}_h} |V| \phi(u_V^n) u_V^-, \end{aligned}$$

where we have introduced the notations:

$$\phi(u_V^n) := \tau_n f_V(u_V^n) + u_V^n$$

and

$$(u_V)^- := \max(0, -u_V),$$

that gives

$$\begin{aligned} \sum_{V \in \mathcal{V}_h} |V| (u_V^-)^2 - \frac{\tau_n}{\varepsilon} \sum_{\gamma \in \mathcal{E}_\gamma} \frac{|\gamma|}{d_\gamma} D_\gamma (u_W - u_V) (u_W^- - u_V^-) \\ = - \sum_{V \in \mathcal{V}_h} |V| \phi(u_V^n) u_V^-. \end{aligned}$$

Bearing in mind that

$$(u_W - u_V) (u_W^- - u_V^-) \leq 0, \tag{10}$$

for all $\gamma \in \mathcal{E}_\gamma$; γ is the common edge for the control volumes V and W .

Using the assumptions (1), (2)-(i), (3) and the non-negativity of $(u_V^n)_{V \in \mathcal{V}_h}; u_V^n \geq 0, \forall V \in \mathcal{V}_h$, we get:

$$\begin{aligned} \phi(u_V^n) &= \tau_n f_V(u_V^n) + u_V^n \\ &\geq (1 - \tau_n \Theta_{u^n, 0}) u_V^n \\ &\geq 0, \end{aligned}$$

for all $V \in \mathcal{V}_h$.

This estimation together with (10) yields

$$\sum_{V \in \mathcal{V}_h} |V| (u_V^-)^2 \leq 0,$$

which leads to $u_V^- = 0, \forall V \in \mathcal{V}_h$. We conclude that $u_V^{n+1} \geq 0, \forall V \in \mathcal{V}_h$ as we wanted to prove.

Unfortunately, we have given a constraint on the time step size limit τ_n^{max} but this one is not a too strong condition in terms of computational cost. This choice can be in range for many two-time reaction-diffusion equations in population dynamics.

The above arguments, with a modification, lead to the following monotonicity result:

Lemma 3. Let Ω be an open polygonal bounded subset of \mathbb{R}^p . Under assumptions (1), (2) and (3) with $\tau_n^{max} = \Theta_{u^n, w^n}^{-1}, \forall n \in \{0, \dots, N-1\}$. Let $(u_V)_{V \in \mathcal{V}_h}$ and $(w_V)_{V \in \mathcal{V}_h}$ be two approximate solutions to (8) corresponding to initial data $(u_V^0)_{V \in \mathcal{V}_h}$ and $(w_V^0)_{V \in \mathcal{V}_h}$ respectively such that $u_V^0 \geq w_V^0, \forall V \in \mathcal{V}_h$. Then,

$$u_V^{n+1} \geq w_V^{n+1}, \forall V \in \mathcal{V}_h \text{ and } \forall n \in \{0, \dots, N-1\}.$$

Proof. Let's assume that $(u_V)_{V \in \mathcal{V}_h}$ and $(w_V)_{V \in \mathcal{V}_h}$ are two approximate solutions to (8) corresponding to initial data $(u_V^0)_{V \in \mathcal{V}_h}$ and $(w_V^0)_{V \in \mathcal{V}_h}$ respectively such that $u_V^0 \geq w_V^0, \forall V \in \mathcal{V}_h$. Then, the vector

$$(y_V)_{V \in \mathcal{V}_h} := (u_V - w_V)_{V \in \mathcal{V}_h}$$

satisfies the following system, together with a non-negative initial data $(y_V^0)_{V \in \mathcal{V}_h} := (u_V^0 - w_V^0)_{V \in \mathcal{V}_h}$,

$$\begin{aligned} |V| y_V^{n+1} - \frac{\tau_n}{\varepsilon} \sum_{\gamma \in \partial V \cap \mathcal{E}_\gamma} \frac{|\gamma|}{d_\gamma} \bar{D}_\gamma (y_W^{n+1} - y_V^{n+1}) &= |V| \Phi(u_V^n, w_V^n), \\ V \in \mathcal{V}_h, n \in \{0, \dots, N-1\}, \end{aligned}$$

where we denote

$$\Phi(u_V^n, w_V^n) := \tau_n (f_V(u_V^n) - f_V(w_V^n)) + u_V^n - w_V^n.$$

Let us assume that $y_V^n \geq 0, \forall V \in \mathcal{V}_h$, and prove that $y_V := y_V^{n+1} \geq 0, \forall V \in \mathcal{V}_h$. For this, we multiply (8) by y_V^- and sum over V , we get:

$$\begin{aligned} \sum_{V \in \mathcal{V}_h} |V| y_V y_V^- - \frac{\tau_n}{\varepsilon} \sum_{V \in \mathcal{V}_h} \sum_{\gamma \in \partial V \cap \mathcal{E}_\gamma} \frac{|\gamma|}{d_\gamma} \bar{D}_\gamma (y_W - y_V) y_V^- \\ = \sum_{V \in \mathcal{V}_h} |V| \Phi(u_V^n, w_V^n) y_V^-, \end{aligned}$$

that gives

$$\begin{aligned} \sum_{V \in \mathcal{V}_h} |V| (y_V^-)^2 - \frac{\tau_n}{\varepsilon} \sum_{\gamma \in \mathcal{E}_\gamma} \frac{|\gamma|}{d_\gamma} D_\gamma (y_W - y_V) (y_W^- - y_V^-) \\ = - \sum_{V \in \mathcal{V}_h} |V| \Phi(u_V^n, w_V^n) y_V^-. \end{aligned}$$

Taking into account that

$$(y_W - y_V) (y_W^- - y_V^-) \leq 0,$$

for all $\gamma \in \mathcal{E}_\gamma$; γ is the common edge for the control volumes V and W .

Using the assumptions (1), (2)-(i), (3) and the non-negativity of $(y_V^n)_{V \in \mathcal{V}_h}; y_V^n \geq 0, \forall V \in \mathcal{V}_h$, we get:

$$\Phi(u_V^n, w_V^n) \geq (1 - \tau_n \Theta_{u^n, w^n}) y_V^n \geq 0,$$

for all $V \in \mathcal{V}_h$.

We proceed in the same manner as in the proof of the previous lemma, we find

$$\sum_{V \in \mathcal{V}_h} |V| (y_V^-)^2 \leq 0,$$

which leads to $y_V^- = 0, \forall V \in \mathcal{V}_h$. We conclude that $u_V^{n+1} \geq w_V^{n+1}, \forall V \in \mathcal{V}_h$.

Now, we can prove the result concerning the boundedness of approximate solution:

Lemma 4. Let Ω be an open polygonal bounded subset of \mathbb{R}^p . Let $(u_V)_{V \in \mathcal{V}_h}$ be an approximate solution to (8) corresponding to non-negative initial data $(u_V^0)_{V \in \mathcal{V}_h}$. Under the assumptions (1), (2), and (3) with $\tau_n^{\max} = \Theta_n^{-1}$ where

$$\Theta_n = \max\{\Theta_{u^n, C}, \Theta_{u^n, 0}\}, \quad \forall n \in \{0, \dots, N-1\}.$$

Then, there exists a positive constant C only depending on u_0 and C_f ; C_f is the constant mentioned in Hypothesis (2)-(ii), such that

$$\sup\{|u_V^{n+1}|, V \in \mathcal{V}_h, n \in \{0, \dots, N-1\}\} \leq C.$$

Proof. Let's assume that $(u_V)_{V \in \mathcal{V}_h}$ is an approximate solution to (8) corresponding to non-negative initial data $(u_V^0)_{V \in \mathcal{V}_h}$ and set

$$C > \max\{C_f, \max\{|u_V^0|, V \in \mathcal{V}_h\}\} > 0,$$

where $C_f > 0$ is the constant mentioned in Hypothesis (2)-(ii). All the assumptions of Lemma 2 are satisfied, and thus its conclusion holds, $|u_V^n| = u_V^n, V \in \mathcal{V}_h, n \in \{1, \dots, N\}$.

We proceed using mathematical induction; clearly $\sup\{u_V^0, V \in \mathcal{V}_h\} \leq C$, for this we assume that $\sup\{u_V^n, V \in \mathcal{V}_h\} \leq C$.

Multiplying in both sides of (8) by

$$(u_V^{n+1} - C)^+ := \max(0, u_V^{n+1} - C)$$

and summing over V , similar calculations to those in the proof of Lemma 1 lead to

$$\begin{aligned} \sum_{V \in \mathcal{V}_h} |V| ((u_V^{n+1} - C)^+)^2 + \frac{\tau_n}{\varepsilon} \sum_{\gamma \in \mathcal{E}_\gamma} \frac{|\gamma|}{d_\gamma} D_\gamma B_\gamma \\ = \sum_{V \in \mathcal{V}_h} |V| \phi(u_V^n) (u_V^{n+1} - C)^+, \end{aligned}$$

where

$$B_\gamma := (u_W^{n+1} - u_V^{n+1}) ((u_W^{n+1} - C)^+ - (u_V^{n+1} - C)^+)$$

and

$$\phi(u_V^n) := \tau_n f_V(u_V^n) + u_V^n - C.$$

Taking into account that

$$B_\gamma \geq 0, \quad \forall \gamma \in \mathcal{E}_\gamma;$$

γ is the common edge for the control volumes V and W . That gives

$$\sum_{V \in \mathcal{V}_h} |V| ((u_V^{n+1} - C)^+)^2 \leq \sum_{V \in \mathcal{V}_h} |V| \phi(u_V^n) (u_V^{n+1} - C)^+.$$

Using the assumptions (1), (2)-(i), (3) and $u_V^n - C \leq 0, \forall V \in \mathcal{V}_h$, we get:

$$\begin{aligned} \phi(u_V^n) &= \tau_n f_V(u_V^n) + u_V^n - C \\ &\leq (1 - \tau_n \Theta_n) (u_V^n - C) + \tau_n f(x_V, C) \\ &\leq 0, \end{aligned}$$

for all $V \in \mathcal{V}_h$, that leads to

$$\sum_{V \in \mathcal{V}_h} |V| ((u_V^{n+1} - C)^+)^2 \leq 0,$$

which gives $(u_V^{n+1} - C)^+ = 0$ and then $u_V^{n+1} \leq C, \forall V \in \mathcal{V}_h$. This completes the proof.

In this work, we have established sufficient conditions to preserve the main features of the approximate solution and ensure L^∞ -stability of semi-implicit finite volume scheme (8) applied to Problem 3. In fact, under the assumptions of Lemma 4, the semi-implicit scheme (8) is conditionally L^∞ -stable according to the existence of a positive constant C only depending on u_0 and C_f such that

$$\sup\{|u_V^n|, V \in \mathcal{V}_h, n \in \{1, \dots, N\}\} \leq C,$$

which means that the approximate solution is bounded in L^∞ by a positive constant independent to the mesh \mathcal{T}_h and the final time T . Therefore, in the scheme (8), no additional hypothesis on the mesh \mathcal{T}_h is required to ensure the L^∞ -stability, which justifies the use of such scheme. Thus, instability phenomenon is only caused by temporal discretization. Moreover, since the constant C is independant of the final time T the global existence of approximate solution is guaranteed.

5 Auto adaptive time step algorithm and numerical results

5.1 Auto adaptive algorithm

Semi-implicit scheme is widely used to find an approximate solution for linear diffusion models in terms of computational cost. In our model, the time step influences the main features of the solution. Indeed, the approximate solution preserves the non-negativity, monotonicity and boundedness of the exact one when time step τ_n is chosen less than τ_n^{\max} at the $(n+1)$ -th iteration. The preservation of each property requires a specific assumption on time step length. Also, an efficient time step control that preserves all the features of the continuous solution is hard to achieve. For this reason, we present in this section a practical algorithm for the numerical implementation of automatic adaptive time step length control. This algorithm will be useful to ensure the L^∞ -stability of the scheme and preserve the most important features; namely the non-negativity and boundedness.

A strategy for controlling the time step length adaptively with semi-implicit finite volume scheme (8) consists of introducing a tolerance parameter θ , $\theta \in]0, 1[$, with a time step size limit τ_n^{max} to control the time step length, at the (n+1)-th iteration. The time step size is proposed to be $\tau_n = \theta \tau_n^{max}$.

The proposed algorithm may be summarized in the following steps:

1. Prepare the pre-processing data such as: space discretization data, initial data, etc...
2. Calculate the time step size limit τ_n^{max} at (n+1)-th iteration using the information at the previous iteration by the formula

$$\tau_n^{max} = (\max\{\Theta_{u^n, C}, \Theta_{u^n, 0}\})^{-1}.$$
3. Choose a value for θ and use $\tau_n = \min\{\theta \tau_n^{max}, \tau\}$ where τ is the desired maximum time step length.
4. Calculate rigidity matrix for the linear system (8) and solve the latter, using the chosen time step length τ_n .
5. Repeat steps 2, 3 and 4.

In step 3, other formula may be introduced if we want to introduce an error time step size control τ_n^{err} in the algorithm, we can set $\tau_n = \min\{\theta \tau_n^{max}, \tau_n^{err}, \tau\}$.

5.2 Numerical results

Under the assumptions (1), (2) and (3), we have shown that the semi-implicit finite volume scheme (8) is L^∞ -stable and it admits a unique approximate solution, even more it preserves the main features of its exact one. In this case, assumptions (1) and (2) ensure the existence and uniqueness of solution to (8), however the additional assumption (3) is used to ensure stability and preserve the non-negativity and boundedness of exact solution.

This work is about investigating the influence of an adaptive time step control on the main features of solutions and the accuracy of simulations. To verify this numerically, we present numerical results for a spatially distributed population growing logistically with fast diffusion. More particularly, we consider the model,

$$\begin{cases} \frac{\partial u}{\partial t}(x, t) = \frac{D}{\varepsilon} \Delta u(x, t) + f(x, u(x, t)), \\ x = (x_1, x_2) \in \Omega =]0, 1[\times]0, 1[, t \in (0, T) \\ \frac{\partial u}{\partial \nu}(x, t) = 0, x \in \partial\Omega, t \in (0, T) \\ u(x, 0) = n_0(x), x \in \Omega \end{cases} \quad (11)$$

where $u(x, t)$ represents the population density at position x and at time t . The reaction term is given by the function f , representing the population growth, defined by

$$f(x, u(x, t)) = r(x)u(x, t) \left(1 - \frac{u(x, t)}{K(x)} \right),$$

where r and K are real-valued continuous functions defined on Ω , $r(x) > 0$ and $K(x) > 0$ for all $x \in \Omega$, which represent respectively the growth rate and the capacity caring of the environment. More precisely, f satisfies Hypothesis 1 and 2. Furthermore, we can easily see that the function h in Hypothesis 1, is given by

$$h(x, u, v) = r(x) \left| 1 - \frac{u + v}{K(x)} \right|.$$

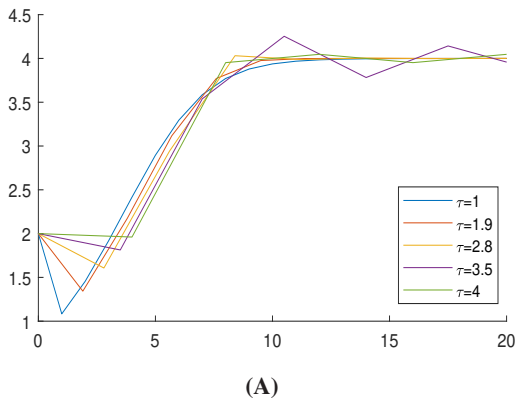
We use the semi-implicit finite volume scheme (8) to give numerical results for (11). We consider triangular mesh of $\Omega =]0, 1[\times]0, 1[$ with maximum edge length $h = 0.05$. We perform the numerical experiments with $\varepsilon = 0.1$ and $D = 0.5$. We denote the monotonicity indicator between $(u_V)_{V \in \mathcal{Y}_h}$ and $(w_V)_{V \in \mathcal{Y}_h}$ at time t_n by

$$Ind_\Omega(t_n) := \min_{V \in \mathcal{Y}_h} (w_V^n - u_V^n),$$

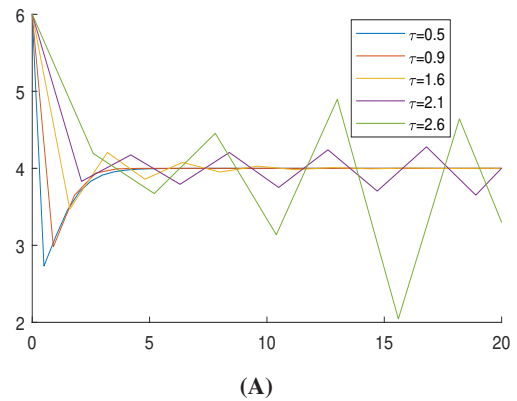
where $(u_V)_{V \in \mathcal{Y}_h}$ and $(w_V)_{V \in \mathcal{Y}_h}$ are two approximate solutions to (11) corresponding to initial data $(u_V^0)_{V \in \mathcal{Y}_h}$ and $(w_V^0)_{V \in \mathcal{Y}_h}$ respectively. Clearly, if $Ind_\Omega(t_n)$ keeps the same sign over time, the monotonicity between $(u_V)_{V \in \mathcal{Y}_h}$ and $(w_V)_{V \in \mathcal{Y}_h}$ is preserved.

Fig. 2 and 3, represent numerical results to (11) using predefined constant time step, and show that the L^∞ -stability of semi-implicit finite volume scheme applied to (11) is not ensured for an arbitrary constant time step length. However, when the time step τ stays below $\tau_{max} = \min\{\tau_{max}^n; n \in \{0, \dots, N\}\}$; $\tau_{max} \approx 2$ in Fig. 2 and $\tau_{max} \approx 0.5$ in Fig. 3, the main features of the approximate solution are preserved. Moreover, we see in Fig. 2-(c) and 3-(c) that $Ind_\Omega(t)$ keeps the same sign over time only if the time step $\tau < \tau_{max}$. Then, in this case, the monotonicity is preserved. Finally, we have confirmed numerically that the approximate solution preserves the non-negativity, monotonicity, and boundedness of its exact one when the time step is chosen less than τ_{max} . Nevertheless, using a fixed time step algorithm, a lot of unnecessary computational work has to be done when τ_{max} is too small.

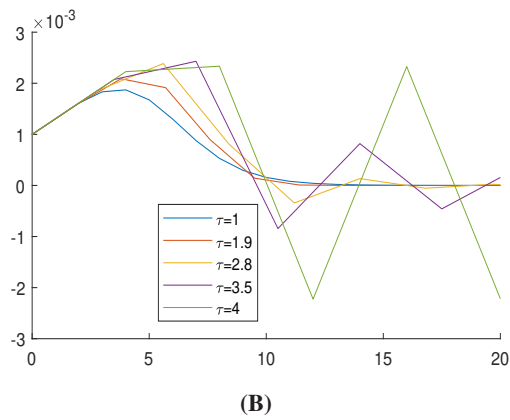
As shown in Fig. 4 and 5, using auto adaptive time-step algorithm, the approximate solution preserves the boundedness and non-negativity of the exact one. In addition, in Fig. 4-(c) and Fig. 5-(c), we present the evolution of the used adaptive time step length that is automatically and entirely determined by the expression of the function h in each iteration. The influence of an adaptive time step algorithm has revealed in the numerical simulations to preserve the main features of the continuous solution, the accuracy of the results, and the efficiency of the simulations in terms of computational cost.



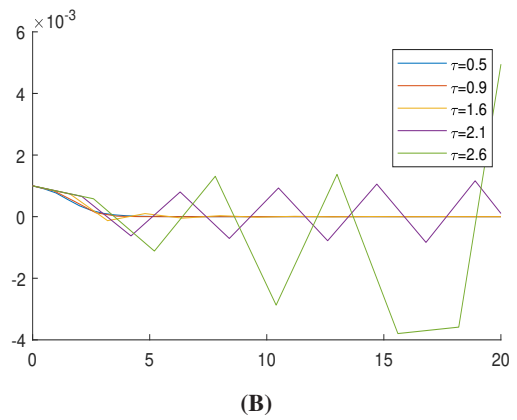
(A)



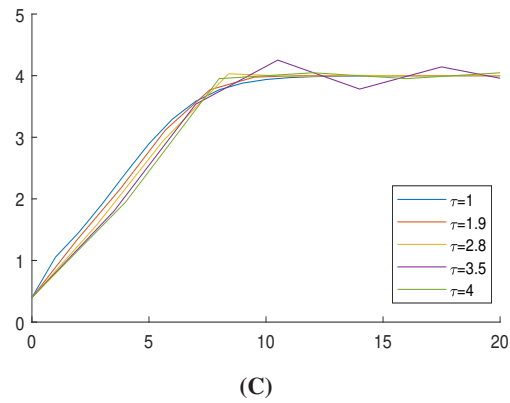
(A)



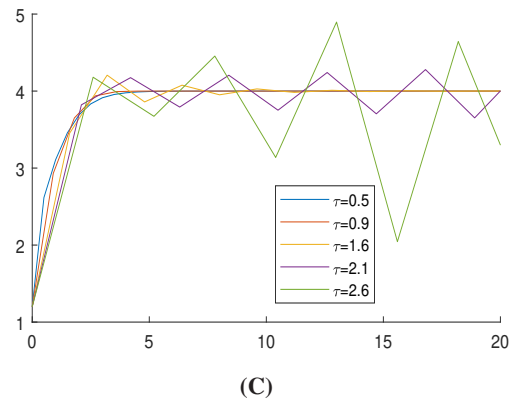
(B)



(B)



(C)



(C)

Fig. 2: Plot of $\max\{u_V, V \in \mathcal{V}_h\}$, (A), $\min\{u_V, V \in \mathcal{V}_h\}$, (B), for the approximate solution corresponding to initial data $u_0(x) = 2(\cos(\pi x_1) + \cos(\pi x_2) + 3)^{-1}$, and the monotonicity indicator $Ind_\Omega(t)$ between the approximate solutions corresponding to initial data u_0 and $w_0 = u_0 + 10^{-3}$, (C), with respect to time t for different values of constant time step τ where $r = 0.5$ and $K = 4$.

Fig. 3: Plot of $\max\{u_V, V \in \mathcal{V}_h\}$, (A), $\min\{u_V, V \in \mathcal{V}_h\}$, (B), and the monotonicity indicator $Ind_\Omega(t)$, (C), with respect to time, using the same parameters as Fig. 2, $r = 1$, and $K = 4$.

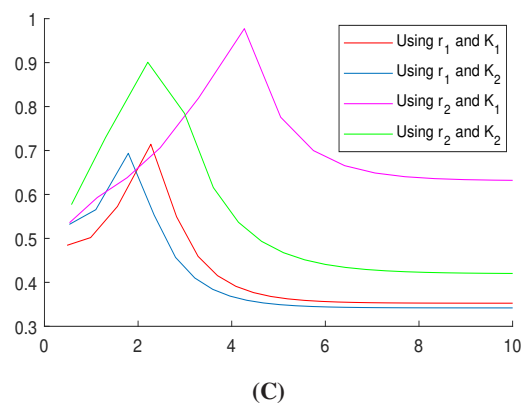
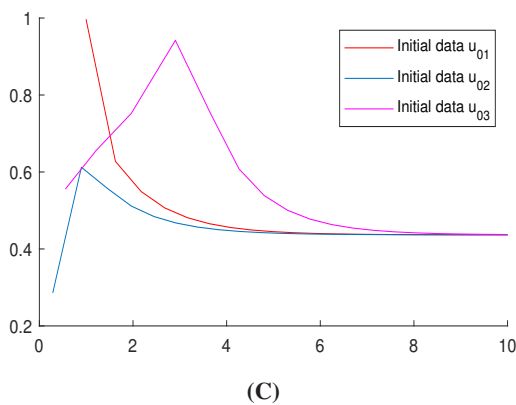
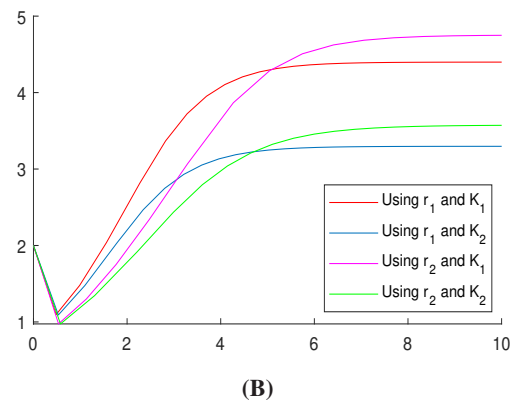
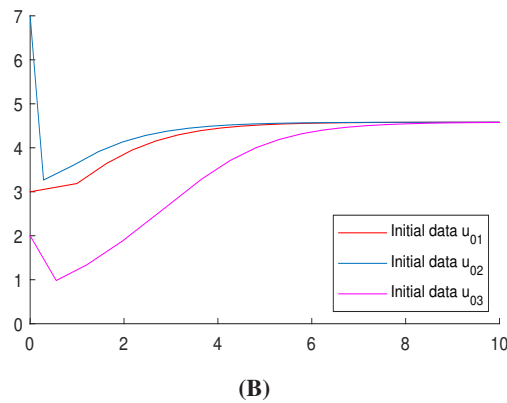
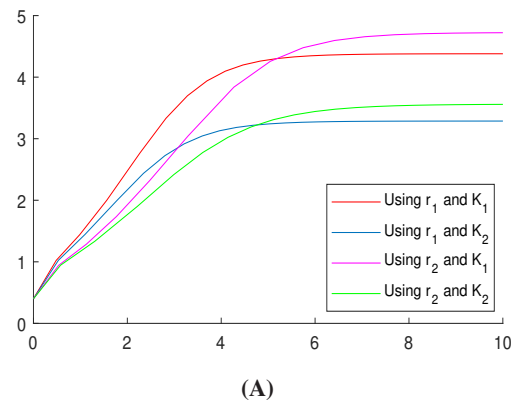
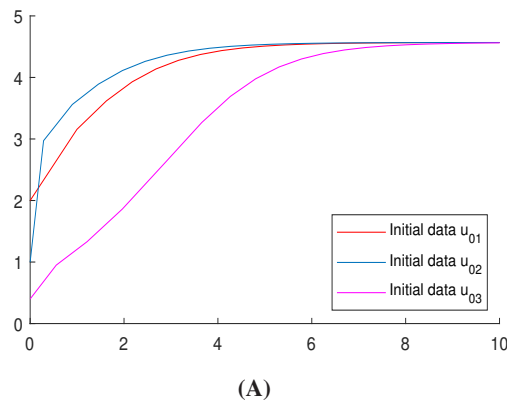


Fig. 4: Plot of $\min\{u_V, V \in \mathcal{Y}_h\}$, (A), and $\max\{u_V, V \in \mathcal{Y}_h\}$, (B), with respect to time for the approximate solution corresponding to different values of the initial data u_0 ; $u_{01}(x) = x_2 \sin(\pi x_1) + 2$, $u_{02}(x) = 4x_1^2 + 2x_2^2 + 1$, and $u_{03}(x) = (x_1 + x_2 + 1)^{-1}$, using auto adaptive time-step algorithm with tolerance parameter $\theta = 0.75$ where $r(x) = x_1 x_2 + 0.5$ and $K(x) = \sin(\pi x_1 x_2) + 4$. In (C) the evolution of the time step length used in auto adaptive algorithm.

Fig. 5: Plot of $\min\{u_V, V \in \mathcal{Y}_h\}$, (A), and $\max\{u_V, V \in \mathcal{Y}_h\}$, (B), with respect to time, corresponding to initial data $u_0(x) = (x_1 + x_2 + 0.5)^{-1}$ for different expressions of functions r and K , $r_1(x) = \sin(\pi(x_1 + x_2)) + 1$, $r_2(x) = x_1 x_2 + 0.5$, $K_1(x) = x_1^2 + x_2^2 + 4$, and $K_2(x) = \sin(\pi x_1 x_2) + 3$. In (C) the evolution of the time step length used in auto adaptive algorithm with $\theta = 0.75$.

6 Conclusion

In this work, we conclude that semi-implicit scheme is L^∞ -stable, and even more it preserves at the discrete level the main features of the continuous problem; namely the non-negativity, monotonicity and boundedness, when the assumptions are satisfied. The numerical study is related to the influence of using an adaptive time step control with respect to computational cost and the accuracy of the results in terms of preserving the main features of the continuous solution. Summarizing, auto adaptive time step algorithm is an effective tool to obtain accurate solutions with less computational cost.

Acknowledgement

The authors are grateful to the anonymous referee for a careful checking of the details and for helpful comments that improved this paper.

References

- [1] J. D. Murray, *Mathematical Biology: I. An Introduction*, Interdisciplinary Applied Mathematics Springer, (2007).
- [2] W. Gurney and R. M. Nisbet, *Ecological dynamics*, Oxford University Press, (1998).
- [3] D. Tilman and P. Kareiva, *Spatial ecology: the role of space in population dynamics and interspecific interactions (MPB-30)*, Princeton University Press, (2018).
- [4] A. Bergam, C. Bernardi, F. Hecht, and Z. Mghazli, Error indicators for the mortar finite element discretization of a parabolic problem, *Numerical Algorithms*, **34**, 187–201, (2003).
- [5] A. Bergam, Z. Mghazli, and R. Verfürth, Estimateurs a posteriori d'un schéma de volumes finis pour un problème non linéaire, *Numerische mathematik*, **95**, 599–624, (2003).
- [6] A. Bergam, C. Bernardi, and Z. Mghazli, A posteriori analysis of the finite element discretization of some parabolic equations, *Mathematics of computation*, **251**, 1117–1138, (2005).
- [7] Z. Mghazli, M. Afif, A. Bergam, and R. Verfürth, A posteriori estimators of the finite volume discretization of an elliptic problem, *Numerical Algorithms*, **34**, 127–136, (2003).
- [8] S. Berrone and M. Marro, Space-time adaptive simulations for unsteady navier–stokes problems, *Computers & Fluids*, **38**(6), 1132–1144, (2009).
- [9] D. Teleaga and J. Lang, Higher-order linearly implicit one-step methods for three-dimensional incompressible navier–stokes equations, *Studia Babes-Bolyai Matematica*, **53**, 109–121, (2008).
- [10] H. W. Alt and S. Luckhaus, Quasilinear elliptic-parabolic differential equations, *Mathematische Zeitschrift*, **183**(3), 311–341, (1983).
- [11] K. Morton and E. SÜLI, Finite volume methods and their analysis, *IMA Journal of Numerical Analysis*, **11**(2), 241–260, (1991).
- [12] R. Eymard, T. Gallouët, and R. Herbin, Finite volume methods, *Hand-book of Numerical Analysis*, P.G. Ciarlet and J.L. Lions eds, North-Holland, **7**, 713–1020, (2000).
- [13] R. Vilsmeier, F. Benkhaldoun, and D. Hänel, *Finite volumes for complex applications II*, Hermes Science Publications, Paris, (1999).
- [14] E. Godlewski and P.-A. Raviart, *Numerical approximation of hyperbolic systems of conservation laws*, Springer Science & Business Media, (2013).
- [15] A. Harten, High resolution schemes for hyperbolic conservation laws, *Journal of computational physics*, **49**(3), 357–393, (1983).
- [16] R. J. LeVeque, *Conservative methods for nonlinear problems*, Springer, (1990).
- [17] P. Auger and R. Bravo de la Parra, Methods of aggregation of variables in population dynamics, *Comptes Rendus de l'Académie des Sciences - Series III - Sciences de la Vie*, **323**(8), 665–674, (2000).
- [18] P. Auger, J. C. Poggiale, and E. Sánchez, A review on spatial aggregation methods involving several time scales, *Ecological Complexity*, **10**, 12–25, (2012).
- [19] E. Sanchez, P. Auger, and J. C. Poggiale, Two-time scales in spatially structured models of population dynamics: A semigroup approach, *Journal of Mathematical Analysis and Applications*, **375**(1), 149–165, (2011).
- [20] C. Bernardi and G. Raugel, Approximation numérique de certaines équations paraboliques non linéaires, *RAIRO. Analyse numérique*, **18**(3), 237–285, (1984).
- [21] J.-L. Lions, *Handbook of numerical analysis*, Elsevier, (2011).



Anouar El Harrak is PhD student at PolyDisciplinary Faculty of Larache, Abdelmalek Essaadi University, Morocco. His research interests are in the areas of applied mathematics and numerical analysis.



Amal Bergam received the PhD degree in Applied Mathematics (Numerical Analysis) and currently working as professor at Department of Mathematics, PolyDisciplinary Faculty of Larache, Abdelmalek Essaadi University, Morocco. Her research interests are in the areas of applied mathematics and numerical analysis (a posteriori error estimate).